International Journal of Modern Physics B
Vol. 30 (2016) 1650205 (20 pages)

DOI: 10.1142/S0217979216502052

Diffusion coefficients of nitric oxide in water: A molecular dynamics study

Sunil Pokharel*, Nurapati Pantha† and N. P. Adhikari‡

Central Department of Physics, Tribhuvan University, Kirtipur, Kathmandu, Nepal
**physicistsupo@gmail.com*
†mrnurapati@gmail.com
‡npadhikari@gmail.com

Received 26 March 2016
Revised 2 June 2016
Accepted 6 June 2016
Published 19 September 2016

Self-diffusion coefficients along with the mutual diffusion coefficients of nitric oxide (NO) and SPC/E water (H_2O) as solute and solvent of the mixture, have been studied within the framework of classical molecular dynamics level of calculations using GROMACS package. The radial distribution function (RDF) of the constituent compounds are calculated to study solute–solute, solute–solvent and solvent–solvent molecular interactions as a function of temperature. A dilute solution of five NO molecules (mole fraction 0.018) and 280 H_2O molecules (mole fraction 0.982) has been taken as the sample. The self-diffusion coefficient of the solvent is calculated by using mean square displacement (MSD) where as that for solute (NO) is calculated by using MSD and velocity auto-correlation function (VACF). The results are then compared with the available experimental values. The results from the present work for water come in good agreement, very precise at low temperatures, with the experimental values. The diffusion coefficients of NO, on the other hands, agree well with the available theoretical studies, and also with experiment at low temperatures (up to 310 K). The results at the higher temperatures (up to 333 K), however, deviate significantly with the experimental observations. Also, the mutual diffusion coefficients of NO in water have been calculated by using Darken's relation. The temperature dependence of the calculated diffusion coefficients follow the Arrhenius behavior.

Keywords: Nitric oxide; diffusion coefficient; molecular dynamics; Arrhenius behavior.

PACS number: 66.10.Cb

1. Introduction

Nitric oxide (NO) is one of the most important signal molecules in a living cell. It is considered as a signal molecule playing a specific role in intracellular and intercellular communication, involves in many physiological and pathological processes.[1] It is a ubiquitous intercellular messenger in vertebrates, modulating blood flow,

thrombosis and neural activity. NO was proclaimed molecule of the year in 1992.[2] In 1998, Nobel Prize in physiology was awarded for the discoveries concerning NO as a signaling molecule in the cardiovascular system. The production of nitric oxide is also important for nonspecific host defense, helping to kill tumors and intracellular pathogens. The biological role of NO as an intracellular messenger molecule mostly depends on the diffusion of NO, which determines its effective concentration in the active cells. The charge neutrality of NO molecule is hydrophobic with respect to aqueous solution which facilitates its free diffusion. When NO molecule is added to aqueous solution, it does not dissolve but instead is excluded by water (H_2O).[3]

Molecular dynamics (MD) simulation has already been considered to be the best alternative for study of system dynamics and structure, which is economical and free from experimental hazards. It can also play an important role of guide to the experimental studies. Nowadays, molecular dynamics tends to become an alternative to experiments in order to provide transport properties.[4] In the recent years, the MD techniques have evolved in the application to macroscopic or real systems to study the complex dynamic processes that occur in biological system like protein stability, protein folding and unfolding, conformational changes, etc. Molecular simulation, which is used to study the time evolution of the system on molecular level to elicit its equilibrium static and dynamic properties, focuses on two most commonly used methods, namely energy minimization and MD that, respectively, optimize structure and simulate the natural motion of biological macromolecules. Molecular motions occur over a wide range of scales in both time and space, and the choice of approach to study them depends on the question asked.[5]

Molecular diffusion occurs as different species of a mixture move under the influence of concentration inhomogeneity.[6] It represents an important role in variety of biospheric and atmospheric sciences. Diffusion is fundamental for transport of matter and for ionic conduction in disordered materials.[7,8] The kinetics of many microstructural changes that occur during preparation, processing and heat treatment of materials include diffusion. The typical examples are nucleation of new phases, diffusive phase transformation, precipitation and dissolution of a second phase, homogenization of alloys, recrystallization and thermal oxidation.[6] The application of diffusion is on integrated circuit fabrication technologies, model processes like chemical vapor deposition (CVD), thermal oxidation and wet oxidation, doping, the operation of solid electrolytes for batteries and fuel cells, surface hardening of steel through carburization or nitridation, etc.[9]

The first attempt to measure self-diffusion (the most basic diffusion process) was that of physico-chemist Georg Karl Von Hevesy who studied self-diffusion in liquid and in solid lead by using a natural radioisotope ^{210}Pb and ^{212}Pb of lead. From the pioneering work of Alder and Wainwright, the simulation of diffusion coefficient has been an area of continuous research. The equations of Fick, the statistical interpretation of diffusion coefficient by Einstein and Smoluchowski and the Boltzmann–Matano method for concentration-dependent diffusion coefficients opened the way for experimental techniques.[10]

2. Diffusion Coefficient

Diffusion is a transport phenomena by which matter is carried from one part of a system to another as a result of random molecular motions. Diffusion coefficient is a response property of the system to a concentration inhomogeneity.[11] When no chemical concentration gradient exists in a system, the molecular displacement are characterized by the corresponding diffusion coefficient called the self-diffusion coefficient.[4] There are two common ways to obtain a self-diffusion coefficient. The first is from the positions of all the molecules present in the system and the second is from velocity of each molecule in the system. The mathematical expression to calculate self-diffusion coefficient from molecular positions is famously known as Einstein relation.[11,12] For 3D system,

$$D = \lim_{t\to\infty} \frac{\left\langle [\mathbf{r}_\alpha(t+t_0) - \mathbf{r}_\alpha(t_0)]^2 \right\rangle}{6t}\,, \tag{1}$$

where α denotes the type of component (solute or solvent) and t_0 is any time origin. The angled brackets $\langle \ldots \rangle$ indicate the ensemble average. The ensemble average is taken over all atoms of the component α in the simulation and all time origins.[13]

The diffusion coefficient calculated using velocities information is known as Green–Kubo formalism, and was first established by Green and Kubo and the relation is[11,12]

$$D_i = \frac{1}{3N_i} \int_0^\infty dt \left\langle \sum_{k=1}^{N_i} \mathbf{v}_i^k(0) \cdot \mathbf{v}_i^k(t) \right\rangle\,, \tag{2}$$

where $\mathbf{v}_i^k(t)$ expresses the velocity vector of molecule k of species i at time t and the notation $\langle \ldots \rangle$ denotes the ensemble average. Equation (2) yields the self-diffusion coefficient for component i averaging over N_i molecules. The Einstein's relationship and the Green–Kubo relationship should give identical results. The term $\langle [\mathbf{r}_\alpha(t + t_0) - \mathbf{r}_\alpha(t_0)]^2 \rangle$ in the Einstein's relation is the mean square displacement (MSD), while the term $\sum_{k=1}^{N_i} \mathbf{v}_i^k(0) \cdot \mathbf{v}_i^k(t)$ in the Green–Kubo relation is usually called velocity autocorrelation function (VACF). The methods using Einstein relation and Green–Kubo relation are, respectively, called as MSD and VACF methods.

In this work, we calculate the self-diffusion coefficients of both the components i.e. NO and H_2O which can be used to estimate the mutual diffusion coefficient using Darken's relation[14]

$$D_{12} = N_2\ D_1 + N_1 D_2\,, \tag{3}$$

where D_1, D_2 are the self-diffusion coefficients of species 1 and 2, respectively and N_1, N_2 are the corresponding mole fractions.

3. Model and Simulation Procedure

3.1. *Modeling of the system*

The simulation has been carried out using MD simulation package GROMACS (GROningen MAchine for Chemical Simulation) 4.6.5. The system under study

consists of five NO molecules and 280 water molecules. The force field used for modeling the system is ffG43a1 (which is inbuilt in GROMACS package). The model of water used for the present study is extended simple point charge (SPC/E). The bond stretching between two covalently bonded atoms i and j is represented by harmonic potential[15]

$$U_b(r_{ij}) = \frac{1}{2}K^b_{ij}(r_{ij} - b_{ij})^2\,, \tag{4}$$

where K^b_{ij} is the force constant and b_{ij} is the equilibrium bond length between two atoms i and j. The bond angle vibration between a triplet of atoms $i-j-k$ is also represented by a harmonic potential on the angle Θ_{ijk}[15]

$$U_a(\Theta_{ijk}) = \frac{1}{2}K^{\Theta}_{ijk}(\Theta_{ijk} - \Theta^0_{ijk})^2\,, \tag{5}$$

where K^{Θ}_{ijk} is the force constant and Θ^0_{ijk} is the equilibrium bond angle. The bonded parameters for NO[3] and water[15] are given in Table 1.

Table 1. Force-field (bonded) parameters for NO molecule and SPC/E water.

	Force constant	Equilibrium bond length and angle	
$K_{\rm NO}$	1.38092×10^5 KJmol^{-1} nm^{-2}	$b_{\rm NO}$	0.115 nm
$K_{\rm OH}$	3.4500×10^5 KJmol^{-1} nm^{-2}	$b_{\rm OH}$	0.1000 nm
$K_{\rm HOH}$	3.8300×10^2 KJmol^{-1} rad^{-2}	Θ_0	109.47°

In Table 1, $b_{\rm NO}$ and $b_{\rm OH}$ are the equilibrium bond length for nitric oxide (N–O) and bond length of oxygen and hydrogen (O–H) in water molecule, respectively. $K_{\rm NO}$ and $K_{\rm OH}$ are the force constants of the bonds N–O in nitric oxide and O–H in water molecule, respectively. Finally, Θ_0 is the equilibrium bond angle (HOH) and $K_{\rm HOH}$ is the strength of the bond angle vibration potential in water molecules. The non-bonded parameters for NO[3] and water[15] are given in Table 2. Here, the subscripts N–N, ON–ON and OW–OW represents the nitrogen–nitrogen interaction in NO molecules, oxygen–oxygen interaction in NO molecules and oxygen–oxygen interaction in water molecules, respectively. The parameters for SPC/E water presented in Table 2 are inherent in GROMACS package. The above parameters in

Table 2. Force-field (non-bonded) parameters for NO molecule and SPC/E water.

NO	Values	Water	Values
$\sigma_{\rm N–N}$	0.3014 nm	$\sigma_{\rm OW–OW}$	0.3165 nm
$\sigma_{\rm ON–ON}$	0.2875 nm		
$\epsilon_{\rm N–N}$	79.54 $k_{\rm B}$	$\epsilon_{\rm OW–OW}$	78.2 $k_{\rm B}$
$\epsilon_{\rm ON–ON}$	96.98 $k_{\rm B}$		

Table 2 are for the Lennard–Jones interaction. In water molecule, the Coulomb interaction arises due to the partial charge of water hydrogen and water oxygen with the values $+0.4238e$ and $-0.8476e$, respectively.[15] Similarly, the Coulomb interaction for NO molecule arises due to the partial charge of oxygen ($-0.0288e$) and nitrogen ($0.0288e$) of NO molecule,[3] where e is the elementary (basic unit of) charge. The intermolecular interaction thus can be written as

$$U_{\alpha\beta}(r_{ij}) = 4\epsilon_{\alpha\beta}\left[\left(\frac{\sigma_{\alpha\beta}}{r_{ij}}\right)^{12} - \left(\frac{\sigma_{\alpha\beta}}{r_{ij}}\right)^{6}\right] + \frac{q_{i\alpha}\, q_{j\beta}}{4\pi\epsilon_0\, r_{ij}}\,, \tag{6}$$

where r_{ij} is the Cartesian distance between the two atoms i and j; α and β indicate the type of the atoms. The parameters for the non-bonded Lennard–Jones interaction between two different atoms are obtained by using Lorentz–Berthelot rule.[15] According to this rule, an arithmetic average is used to calculate $\sigma_{\alpha\beta}$ and a geometric average is used to calculate $\epsilon_{\alpha\beta}$.

$$\sigma_{\alpha\beta} = \frac{1}{2}\left(\sigma_{\alpha\alpha} + \sigma_{\beta\beta}\right) \tag{7}$$

$$\epsilon_{\alpha\beta} = \left(\epsilon_{\alpha\alpha} \times \epsilon_{\beta\beta}\right)^{\frac{1}{2}}\,. \tag{8}$$

3.2. *Simulation procedure*

MD simulation was carried out in a cubic box with dimensions of 2.2 nm with periodic boundary conditions[12] using GROMACS 4.6.5. After solvation, addition of 280 water molecules and five NO molecules in simulation box, energy minimization is carried out with a cutoff restriction of 1.0 nm to avoid unphysical van der Waals

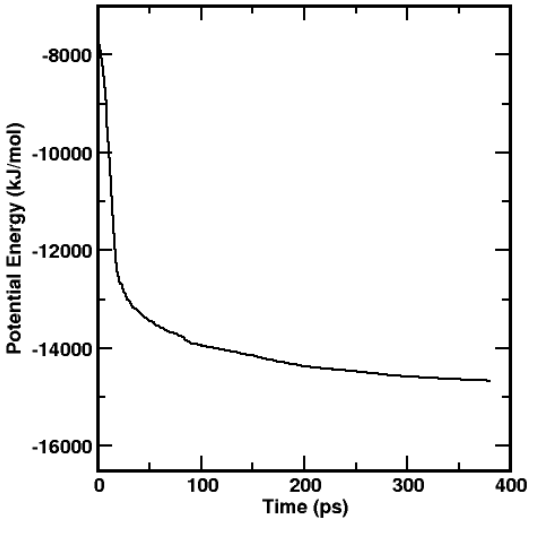

Fig. 1. Plot of potential energy as a function of time after energy minimization.

contact caused by the atoms that are too close.[15] Energy minimization brings the system to equilibrium configuration, removes all the kinetic energy from the system, reduces thermal noise in structure and brings the system to one of the local minimum. Steepest descent algorithm has been used for energy minimization and the algorithm stops when the maximum of absolute value of force components is smaller than the specified value.[15] The energy (potential) of the system after energy minimization is shown in Fig. 1.

After energy minimization, equilibrium was carried out at different temperatures, 293 K, 298 K, 303 K, 310 K, 313 K, 323 K, 333 K and a pressure of 1 bar (i.e. NPT ensemble) by using *velocity-rescaling* thermostat and Berendsen barostat[15] at a coupling time $\tau_t = 0.01$ ps and $\tau_p = 0.6$ ps, respectively. Here, the system is subjected to NPT ensemble to bring the parameters like temperature, pressure, density, etc. to thermodynamic equilibrium because dynamic property like diffusion coefficient varies with such parameters. The system was equilibrated for 200 ns with the time-step of 2 fs and leap-frog algorithm as an integrator. The velocity is generated initially according to a Maxwell distribution function at a specified temperature.[15] All the bonds are converted to constraints using SHAKE algorithm.[15] During equilibration short-range coulomb interaction and Lennard Jones interaction each with a cutoff parameter of 1.0 nm were considered with periodic boundary conditions.[12] The long range Coulomb interaction is handled via the PME algorithm. The input parameters (force-field parameters, and coupling constants for barostat and thermostat) were taken so as to be consistent with the experimental values as much as possible. The structure of the system after equilibration is shown in Fig. 2. The density and simulated temperatures at different coupling temperatures are shown in Table 3.

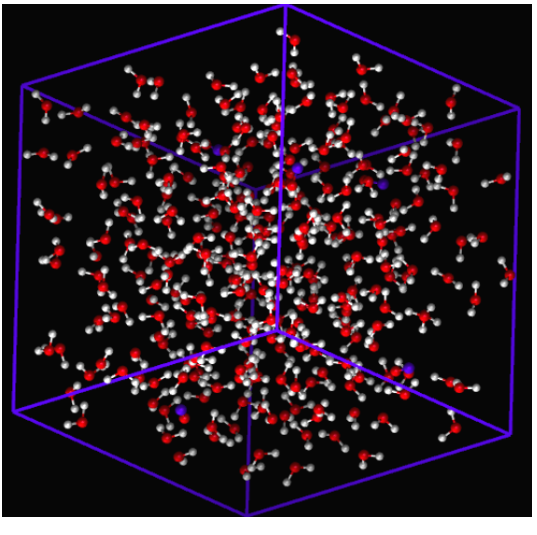

Fig. 2. Structure after equilibration.

Table 3. Values of simulated temperature (T_{sim}) and density at various coupling temperatures (T_{NO}).

S.N	(T_{NO}) K	(T_{sim}) K	ρ_{system} (kg/m^3)	ρ_{water} (kg/m^3)[3,10,16]
1	293	292.970 ± 0.017	994.817 ± 0.045	998.19
2	298	297.967 ± 0.012	992.071 ± 0.025	997.30
3	303	302.957 ± 0.008	989.065 ± 0.026	995.61
4	310	309.959 ± 0.006	984.596 ± 0.041	994.20
3	313	312.956 ± 0.006	982.559 ± 0.007	992.17
4	323	322.955 ± 0.004	975.513 ± 0.024	987.99
5	333	332.967 ± 0.005	967.804 ± 0.031	983.16

Table 3 shows that our simulated value of system density is in maximum deviation of around 1% with that of water density. After equilibration run we perform the production run to calculate the equilibrium properties of the system such as diffusion coefficient by fixing the number of particles, volume and temperature i.e., NVT ensemble. We use *velocity-rescale* thermostat for this case. We do not couple the system to a fixed pressure and use the structure obtained after equilibration run by which we fix the volume of the system. The production run was carried out for 200 ns with the time-step of 2 fs.

3.3. *Energy profile*

Figure 3 represents the energy profile of the system at 303 K with the contributions of different energies. In our force field, total potential energy is the sum of Lennard–

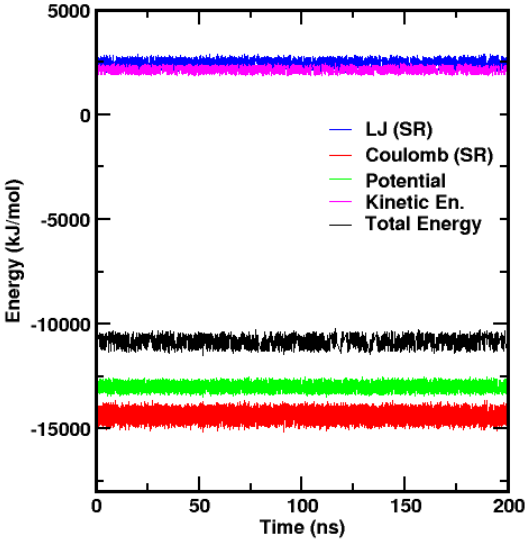

Fig. 3. Energy profile of the system at $T = 303$ K.

Jones and Coulomb energy. As we have used the cutoff values for Lennard–Jones and Coulomb potential the energy corresponding to them are the short-range energies. The total energy is the sum of potential and kinetic energies. The Lennard–Jones interaction energy is positive with an average of 2474.50 ± 0.22 KJ mol^{-1}. The Coulomb energy is negative with value of -14427.80 ± 0.56 KJ mol^{-1} so the potential energy, which is the sum of Lennard–Jones and Coulomb energy is negative with value of -13018.20 ± 0.39 KJ mol^{-1}. The Lennard–Jones energy is positive which destabilizes the system, the attractive Coulomb interaction keeps the system bound and stable. This shows that the dominating part potential energy is Coulomb energy. The kinetic energy is 2143.84 ± 0.05 KJ mol^{-1}, so the total energy, sum of potential and kinetic energy is -10874.40 ± 0.42 KJ mol^{-1}. The negative value of the total energy shows that the system is bounded and is in stable equilibrium.

4. Results and Discussion

In this section, we present and discuss the structural and dynamical properties by studying the radial distribution function (RDF) and diffusivity of solute (NO) and solvent itself, respectively, in SPC/E model of water.

4.1. *Radial distribution function*

We have used radial distribution function (RDF) to evaluate the structure of the system. RDF gives the idea of distribution of neighboring molecules with respect to the reference molecule considered in the calculations. In periodic systems, RDF shows sharp peaks and troughs up to infinity where the separations and heights are the characteristics of the lattice structure. In liquids however, RDF oscillates up to certain orders and then attains constant value as unity.[17]

We have obtained RDF $g(r)$ of oxygen atoms of water molecules $g_{\text{OW–OW}}(r)$, oxygen of water and oxygen of nitric oxide $g_{\text{ON–OW}}(r)$ and also oxygen atoms of nitric oxide themselves $g_{\text{ON–ON}}(r)$. Due to the dominant repulsive part of Coulomb interaction force incorporated by r^{-12} term of Lennard–Jones potential in the calculations, the RDF vanishes at distances $r \to 0$. The region from $r = 0$ to the certain point up to which RDF becomes zero is defined by "excluded region". Physically, the excluded region is the result of presence of hard cores of interacting particles which is observed as excluded volume in spacial distribution of the particles.

Beyond the excluded region, the RDF increases and then oscillates between the peaks and troughs indicating that the distribution of molecules around the reference particle is not uniform. The first peaks in the figures imply the position of nearest neighbors which lie within the first shell. The troughs then imply the absence of particles up to second peak positions. Similarly, the second peaks signify the position of second nearest neighbors defined by next shell, and so on. After few oscillations, $g(r)$ attains its value as unity and fairly remains constant up to ∞. This means that the molecules are not correlated at long distance which is consistent with the established property of other liquid molecules.

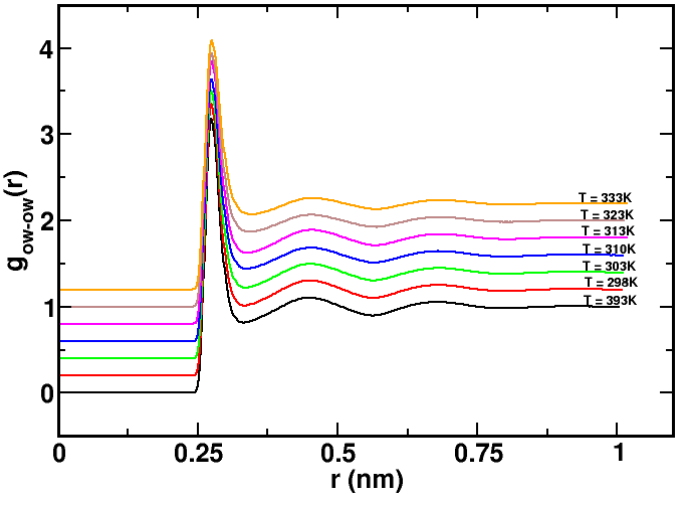

Fig. 4. RDF of oxygen atoms of water molecules at different temperatures.

Table 4. Simulated data for the RDF analysis between the solvent molecules.

	RDF analysis of OW–OW						
T (K)	ER (nm)	FPP (nm)	FPV	SPP (nm)	SPV	TPP (nm)	TPV
293	0.246	0.274	3.181	0.452	1.107	0.680	1.063
298	0.244	0.274	3.156	0.452	1.108	0.682	1.056
303	0.246	0.274	3.105	0.454	1.101	0.682	1.057
310	0.244	0.274	3.054	0.454	1.093	0.684	1.049
313	0.246	0.276	3.020	0.456	1.094	0.686	1.042
323	0.246	0.276	2.952	0.456	1.070	0.690	1.044
333	0.246	0.276	2.900	0.460	1.080	0.692	1.038

ER – excluded region, FPP – first peak position, FPV – first peak value, SPP – second peak position, SPV – second peak value, TPP – third peak position, TPV – third peak value.

Figure 4 represents the RDF of oxygen atoms of water molecules at different temperatures. The figure explores three different peaks which implies that the molecules are correlated up to third solvation shell. The detail of the structural properties is provided in Table 4.

The value of σ for OW–OW is 0.3165nm, and the van der Waals radius ($2^{1/6}\sigma$) is 0.3553 nm.[15] Table 4 shows that excluded region remains fairly independent (0.244 $\pm$ 0.002 nm) of changing temperature. It also calculates that the excluded region is smaller than the van der Waals radius which indicates the contribution from other potentials in addition to the van der Waals potential (see Fig. 5). The first peak position remains at the same position within the error of $\pm$ 0.002 nm as a function of temperature. On the other hand, SPP and TPP shift towards right on

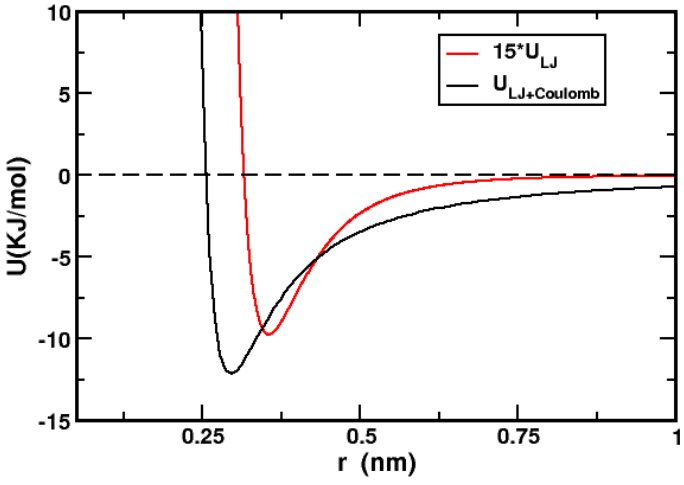

Fig. 5. Lennard–Jones (U_{LJ}) and Lennard–Jones plus Coulomb ($U_{LJ+Coulomb}$) potential as a function of distance for two different isolated water molecules.

increasing temperature. The magnitudes of all the peaks decrease on rising temperature. Furthermore, the width of the peaks increases on increasing temperature. Both variations are the consequences of excess volume created in the system and the decrease in co-ordination number with increase in temperature. These results conclude that the movement of the particles enhances and the solvent becomes less structured as the temperature is increased.

The study of Fig. 5 taken for two isolated molecules, clears that minimum potential is obtained at the shorter distance when both the potentials, Lennard–Jones and Coulomb, are taken into account. As FPP is slightly smaller than the minimum of Fig. 5, Lennard–Jones plus Coulomb potential covers almost entire potential except many body effects. The RDF between the oxygen of water and oxygen of NO describes solute–solvent interaction which widens the horizon of the study, Fig. 6.

Table 5. Simulated data for the RDF analysis between oxygen atom of NO molecule and oxygen atom of water molecule.

RDF analysis of ON–OW					
T(K)	ER (nm)	FPP (nm)	FPV	SPP (nm)	SPV
293	0.258	0.338	1.536	0.664	1.058
298	0.258	0.338	1.510	0.668	1.053
303	0.258	0.343	1.477	0.676	1.052
310	0.258	0.342	1.465	0.670	1.051
313	0.256	0.346	1.425	0.674	1.043
323	0.258	0.340	1.441	0.676	1.047
333	0.256	0.340	1.400	0.678	1.043

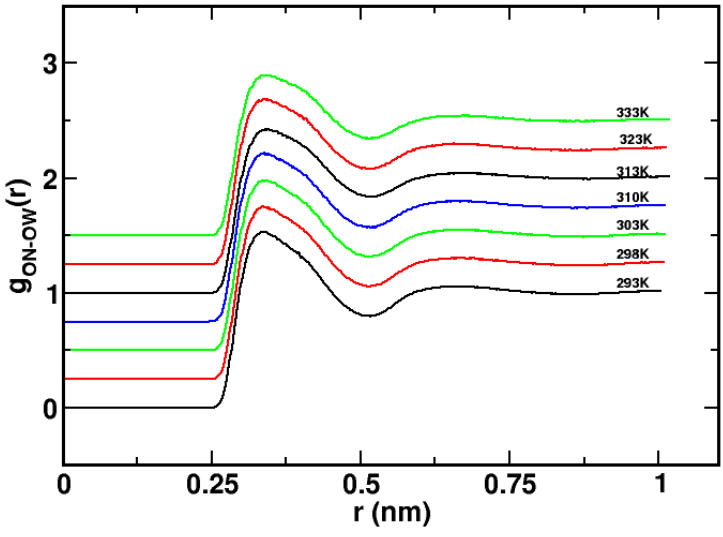

Fig. 6. RDF of oxygen atom of NO molecule and oxygen atom of water molecule at different temperatures.

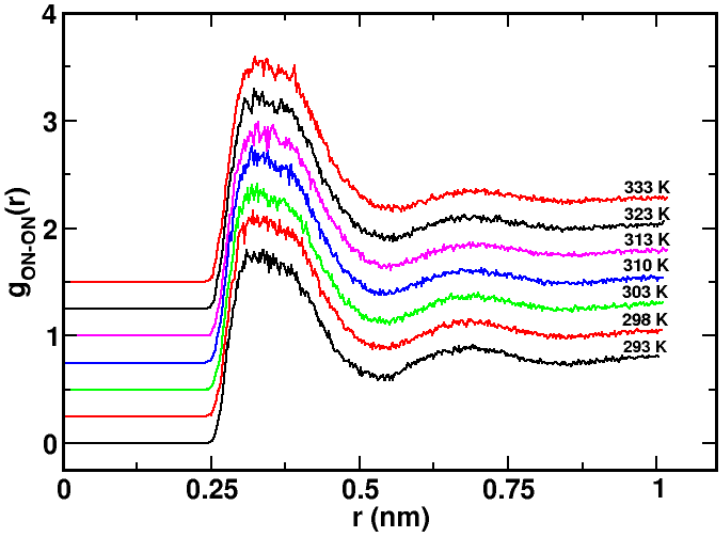

Fig. 7. RDF between oxygen atoms of NO molecule at different temperatures.

The detail of Fig. 6 is given in Table 5. We have observed only two peaks in RDF between the solute and solvent. The magnitudes on Table 5 shows that the excluded region remains almost fixed (with the error of ± 0.004 nm) with varying temperature. Both the peak positions, FPP and SPP, shift slightly to the right on elevating temperature. The peak values on the other hand decrease on rising

Table 6. Simulated data for the RDF analysis between oxygen atoms of NO molecule.

RDF analysis of ON–ON					
T(K)	ER (nm)	FPP(nm)	FPV	SPP(nm)	SPV
293	0.248	0.312	1.796	0.668	0.930
298	0.246	0.318	1.914	0.684	0.908
303	0.246	0.318	1.909	0.701	0.894
310	0.246	0.318	2.009	0.706	0.871
313	0.248	0.330	1.986	0.686	0.869
323	0.246	0.322	2.051	0.676	0.871
333	0.244	0.324	2.090	0.675	0.865

temperature. It again signifies that correlation between NO and water decreases on increasing temperature. The value of σ for ON–OW is 0.30895 nm, and the van der Waals radius ($2^{1/6}\sigma$) is 0.34678 nm.[3,15] It shows that the van der Waals radius is greater than both the FPP (0.338 nm) and excluded region (0.256 nm).

Figure 7 represents the RDF of oxygen atoms of NO molecules. The details of Fig. 7 is given in Table 6. The value of $\sigma_{\text{ON–ON}}$ is 0.2875 nm and the value of van der Waals radius is 0.32271 nm. The excluded region is less than van der Waals radius and first peak position is nearly equal to van der Waals radius. The roughness in the figure (7) is due to the less statistics (only five NO molecules).

4.2. *Diffusion coefficients*

The self-diffusion coefficient of nitric oxide is determined by using Einstein's relation (MSD method) and Green–Kubo formula (VACF method) where as that of water is calculated using MSD method only.

Figure 8 shows the variation of diffusion coefficient $D = \langle r^2(t)\rangle/6 * t$ with time for NO at temperature $T = 303$ K. From Fig. 8 we can say that it is justifiable to take time to 2 ns while calculating diffusion coefficient as the graph is straight up to 2 ns. At first the diffusion coefficient is high due to ballistic motion and later as time passes it remains constant. This constant portion of the graph gives the diffusion coefficient. The ballistic region is also seen in Fig. 9 which is the log–log plot of mean square displacement (MSD) with time and is represented by the parabolic region of the graph very close to origin. In this case, the molecules at the beginning move swiftly in the holes present in the system thereby showing higher value of diffusion coefficient. After certain time the molecules show uniform motion as a result of which we see the linear portion of the plot.

To obtain diffusion coefficient via MSD, we plot the graph between MSD with time. Figures 10 and 11 show the MSD plot of NO and water at different temperatures, respectively. Since the statistics is better due to higher averaging at the starting than towards the ending region, we take the certain portion which has the

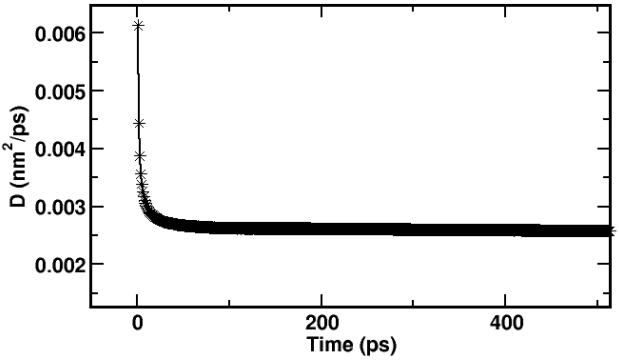

Fig. 8. Plot of diffusion coefficient $D = \langle r^2(t)\rangle/6\ t$ versus time of NO at 303 K.

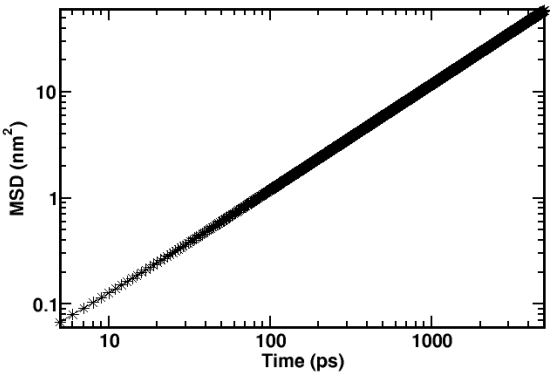

Fig. 9. MSD versus time plot in logarithmic scale for NO at 303 K.

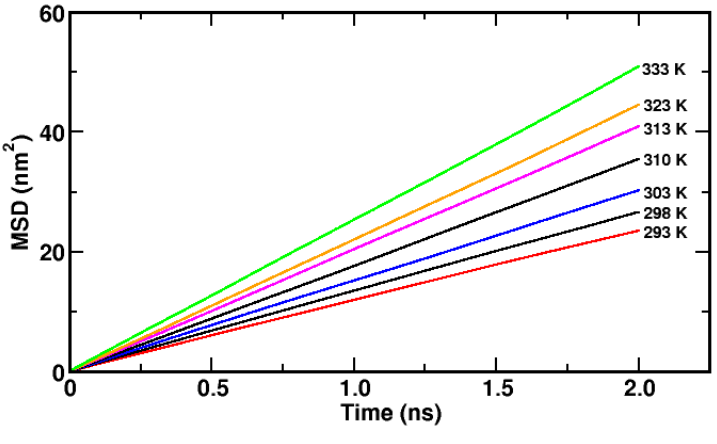

Fig. 10. Plot of MSD versus time of NO at different temperatures.

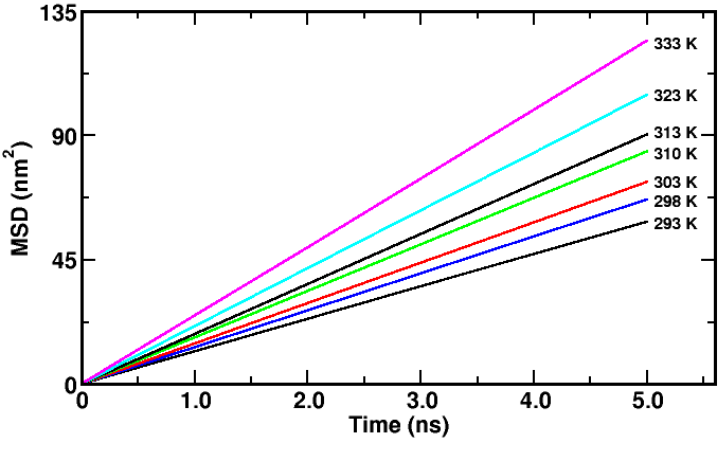

Fig. 11. Plot of MSD versus time of water at different temperatures.

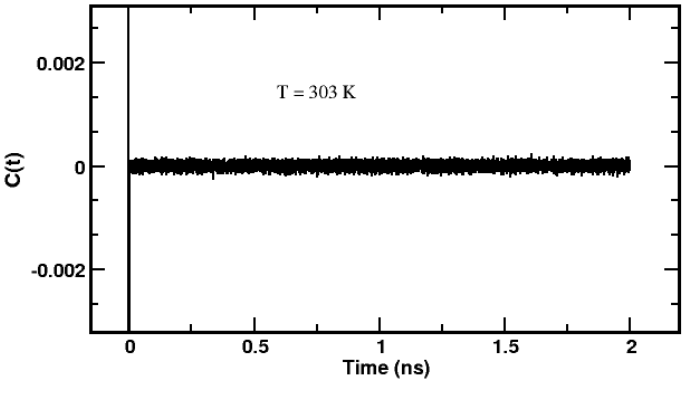

Fig. 12. Plot of $C(t) = \langle v_i(t) \cdot v_i(0) \rangle_{i \in \alpha}$ versus time.

best statistics. We fit the data linearly using *grace*, the slope divided by 6 [Eq. (1)] gives the value of diffusion coefficient of the desired species under study. In our case, we have a simulation time of 200 ns and the best statistics for NO molecule is found within 2 ns which can also be justifiable from Fig. 8 and is very small in comparison to simulation time this is due to lesser number of NO molecules. For water molecule, best statistics is found within 5 ns due to larger number of water molecules. The values of the self-diffusion coefficient of NO and water obtained from MSD plot are presented in Table 7.

Figures 12 and 13 show the variation of velocity autocorrelation function (VACF) with time and the normalized truncated graph to few ps time to see the variation of the velocity correlation function at small time interval for NO at temperature $T = 303$ K. We here look at the product of the two velocities at two instance that are apart by time t. If t is very small, the velocity does not change

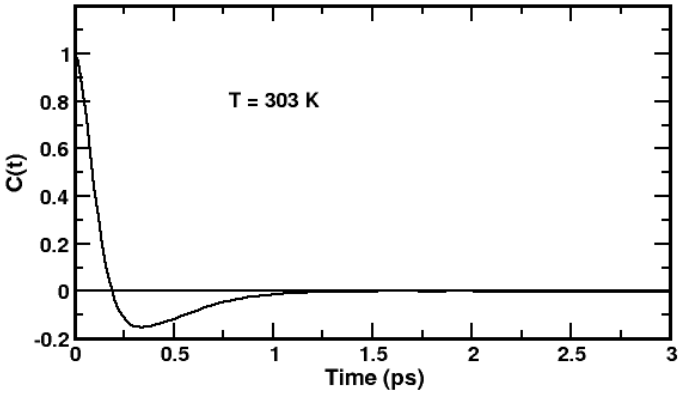

Fig. 13. Plot of normalized $C(t)$ versus time.

Table 7. The simulated value of self-diffusion coefficient of NO and H_2O, and also the references for them as a function of temperature are listed. The mutual diffusion coefficients between the solute and solvent molecules are also mentioned.

	Diffusion coefficient (1×10^{-9} m^2s^{-1})					
	For NO			For H_2O		
Temperature K	MSD	VACF	Ref.	MSD	Ref.	Mutual diffusion
293	2.28	2.31	2.07(a)	1.98	2.02(b)	2.27
298	2.54	2.58	2.21(c)	2.21	2.24(e)	2.53
303	2.73	2.73	3.96(a)	2.42	2.59(b)	2.72
310	3.05	3.06	3.00(c)	2.80	–	3.04
			3.30(d)			
313	3.31	3.46	5.16(a)	3.01	3.24(b)	3.30
323	3.87	4.06	9.34(a)	3.60	3.96(b)	3.86
333	4.66	4.60	13.6(a)	4.33	4.77(b)	4.65

(a) Ref. 18, (b) Ref. 20, (c) Ref. 21, (d) Ref. 22 and (e) Ref. 4.

very much. So, in the limit of small time t, the velocity at time 0 and the velocity at time t are going to be very similar, we can say that there is a correlation. As we move away in time, there is going to be no correlation. The velocity at time 0 and the velocity at an instant that is very far away in time is not going to be correlated. To calculate the self-diffusion coefficient, we integrate the graph (12) and divide the result by three [Eq. (2)]. The comparison of the values obtained by using VACF method, MSD method and the references is shown in Table 7.

The mutual diffusion coefficient is estimated using Darken's relation [Eq. (3)]. Our system consists of five NO and 280 water molecules so the mole fraction for water is 0.982 and that of NO is 0.018. The values of the mutual diffusion coefficient obtained using Eq. (3) is also presented in Table 7.

Table 7 shows the self-diffusion coefficients of NO and H_2O molecules from the present work along with the references and also reveals the mutual diffusion

coefficients between them, at different temperatures. The comparison of the values from the table and also from other references explores that self-diffusion coefficients of water from the present work, in general, come in very good agreement with the previous studies.[3,4,10,20,23] The experimental and simulated values of self-diffusion coefficients are in good agreement with maximum deviation of 9.22% at 333 K.[20] The simulated values of NO, on the other hands, show different attitude towards the references. They agree very well with the experiment performed by Zacharia *et al.*[21] at 298 K and 310 K, which represent the environmental temperature and temperature of physiological importance, respectively. The diffusion coefficient of NO at 310 K also falls within 2% of the experimental work reported by Malinski *et al.*.[22] This trend of agreement is also true with the pioneer work performed by Wise and Houghton (cited in the Table 7, Ref. 18) at low temperature (within 9.21% at 293 K). However, the agreement with the Ref. 18 remains no longer true as we move towards higher temperatures. The values presented by the authors at higher temperatures are abnormally high with reference to the present work and also with other similar molecules (by size and weight, diffusivity is sensitive to these parameters) like carbon monoxide (CO) and molecular oxygen (O_2) mentioned by the same author/s.[18,19] The authors in the paper, claim that the higher diffusivity of NO can be described on the basis of their paramagnetic behavior, which, so far in our knowledge, has not been mentioned by the following research works and also has not been incorporated in the present work which demands further work. Moreover, we have taken the Lennard–Jones optimized parameter at low temperatures.[3]

The diffusion coefficients of NO are obtained by two different methods; VACF and MSD. Table 7 shows that both the methods produce similar values, within maximum deviation of 5.0%. The diffusion coefficient for both the solute and solvent molecules increases with the enhanced temperature, which is due to the increase in the velocity of the molecules, as per relation of the thermal energy with temperature. Furthermore, as the density of the system decreases with increasing temperature, the space available for the nitric oxide molecules to execute random-walk motion increases.[4] Finally, based on these facts, the MSD increases and this change is incorporated by Einstein's relation to yield an increased self-diffusion coefficient. The RDF of oxygen atoms of nitric oxide themselves $g_{\mathrm{ON\text{–}ON}}(r)$ (Fig. 7) shows finite density of the particles in the region between the first and second peaks, which also hints the diffusion process of the molecules in the whole system.

The mutual diffusion coefficient is calculated using Darken's relation [Eq. (3)] and is very close to that of self-diffusion coefficient of solute in the mixture due to low solute concentrations studied in this work.

5. Temperature Dependence

Diffusion generally depends strongly on temperature, being low at low temperatures and significant at high temperatures. The temperature dependence of diffusion coefficients is frequently, but by no means always, found to obey the Arrhenius

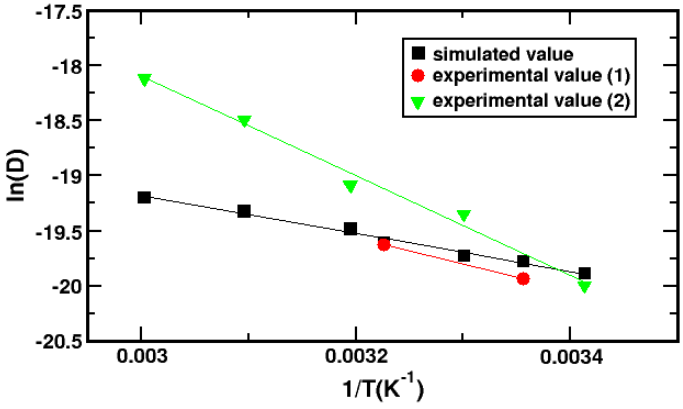

Fig. 14. Arrhenius diagram of the simulated (using VACF method) and experimental value of nitric oxide.

formula[6]

$$D = D_0 \ \exp\left(\frac{-E_a}{N_A k_B T}\right), \tag{9}$$

where D_0 denotes the pre-exponential factor, also called frequency factor, E_a is the activation energy for diffusion, T is the absolute temperature, N_A is Avogadro constant whose value is 6.023×10^{23} and k_{B} is the Boltzmann constant whose value is $1.38 \times 10^{-23}\ JK^{-1}$. Both E_a and D_0 are called the activation parameters of diffusion. The activation energy of diffusion process[6]

$$E_a = -N_A k_B \frac{\partial \ln D}{\partial(1/T)} \tag{10}$$

corresponds to negative slope of the Arrhenius diagram. The intercept of the extrapolated Arrhenius line for $T^{-1} \Longrightarrow 0$ yields the pre-exponential factor D_0. In an Arrhenius diagram, the logarithm of the diffusivity is plotted versus the reciprocal of absolute temperature.

Figure 14 shows the temperature dependence of diffusion coefficient of nitric oxide in water. As the simulation and experimental data fit to Eq. (9), the temperature dependence of diffusion coefficient follows Arrhenius behavior. From Fig. 14, it is clear that there is a good agreement between experimental[21] and simulation results at low temperatures. Further, it is seen that the diffusion coefficients increase with increase in temperatures. This could be due to the fact that at higher temperature the difference in the density of the system (i.e., nitric oxide and water) and water increases with increase in temperature (see Table 3). Moreover, the experimental data[18] have error of 7%. The difference in simulated and experimental values of diffusion coefficient demands more precise experiments to determine diffusion coefficient of nitric oxide in water. Further investigation of diffusion coefficients using *ab initio* molecular dynamics is beyond the scope of the present work.

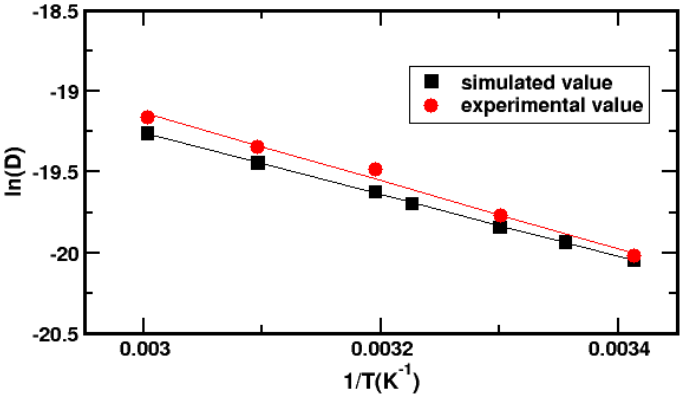

Fig. 15. Arrhenius diagram of the simulated and experimental value of water.

Table 8. Calculation of activation energy.

	Estimation of activation energy in $KJmol^{-1}$		
NO	Activation energy	Water	Activation energy
MSD (NO)	14.28	MSD (Water)	15.87
VACF (NO)	14.32		
Experimental (NO)	19.50	Experimental (Water)	17.43

Figure 15 shows that the temperature dependence of diffusion coefficient of water in the system containing water and nitric oxide. Figure 15 explicitly shows the temperature dependence of diffusion coefficient of water also follows Arrhenius behavior.

We have plotted the Arrhenius diagram and estimated the activation energy for diffusion shown in Table 8. The experimental values in Table 8 are the values obtained by using the experimental data, for Arrhenius diagram and calculating activation energy from it.

6. Conclusions and Concluding Remarks

In this work, we took the system containing 280 water (H_2O) molecules and five nitric oxide (NO) molecules and diffusion of nitric oxide in water for various temperatures 293, 298, 303, 310, 313, 323 and 333 K has been carried out using MD simulation technique. The extended simple point charge (SPC/E) model of water was used. Here nitric oxide (NO) acts as a solute and water (H_2O) as a solvent. The energy profile (Fig. 3) of the system were studied to know the equilibrium nature of the system.

Structural properties has been studied using radial distribution function (RDF), which shows the system becomes less structured at high temperatures. The equilibrium structural properties of both the components (NO and H_2O) were studied

calculating corresponding radial distribution function (RDF) namely $g_{\text{OW–OW}}(r)$ RDF of oxygen atoms of water molecules, $g_{\text{ON–OW}}(r)$ RDF of oxygen atom of NO and oxygen atom of H_2O, $g_{\text{ON–ON}}(r)$ RDF of oxygen atoms of NO molecules. The RDF of $g_{\text{ON–ON}}(r)$ showed some convolutions and depression at short distance due to less number of NO molecules.

The main aim of our work was to study diffusion phenomenon of the mixture of water and NO and study its temperature dependence. The self-diffusion coefficients of water was estimated using Einstein's method and that of NO was estimated using Einstein's and velocity autocorrelation method separately. The values of diffusion coefficients of NO at low temperature agree well with the experimental results.[21] But, the values of diffusion coefficient of NO up to 313 K is deviated within 32.94% of the available experimental data,[18] and that at higher temperature, it reaches up to 65.7% at 333 K. The diffusion coefficients of water are deviated within 9.22% of the available experimental data.[20] The values of the self-diffusion coefficient for NO obtained using MSD and VACF varies within 5%. The binary or mutual diffusion coefficient of the system was calculated using Darken's relation. The Arrhenius diagram (plot of natural logarithm of diffusion coefficient versus inverse of temperature) was plotted for self-diffusion coefficients of NO and H_2O separately and it showed temperature dependence of self-diffusion coefficient of both are of Arrhenius type.

It can, therefore, be concluded that classical molecular dynamics simulation technique can be used as a reliable method to study the equilibrium structure and dynamic properties of fluid mixture. The calculated values of the diffusion coefficient may be used as a reference for any further fluid studies. In the near future, we want to study the diffusion coefficients by varying concentration of the component over wide range of temperature and also want to study the dynamics of other gaseous system.

Acknowledgments

We acknowledge the partial support from The Abdus Salam International Centre for Theoretical Physics (ICTP) through the office of external activities within Net-56. We also appreciate TWAS research grants. Further, N. Pantha acknowledges the partial financial support from Nepal Academy of Science and Technology (NAST), Nepal.

References

1. Y. C. Hou, A. Janczuk and P. G. Wang, *Curr. Pharm. Des.* **5**, 417 (1999).
2. E. Culotta and De Koshland Jr., *Science* **258**, 1862 (1992).
3. Z. Zhou et al., *J. Chem. Phys.* **123**, 054505 (2005).
4. S. K. Thapa and N. P. Adhikari, *Int. J. Mod. Phys. B* **27**, 1350023 (2013).
5. H. B. Moktan, A. Panday and N. P. Adhikari, *Int. J. Mod. Phys. B* **26**, 1250016 (2012).

6. H. Mehrer, *Diffusion in Solids* (Springer Series in Solid State Science, Berlin, 2007), p. 155.
7. V. A. Hermandaris et al., *Macromolecules* **40**, 7026 (2007).
8. N. P. Adhikari et al., *Phys. Rev. Lett.* **93**, 188301 (2004).
9. H. Mehrer and N. A. Stolwijik, *Heroes and Highlights in the History of Diffusion*; Open-Access Journal for the Basic Principles of Diffusion.
10. I. Poudyal and N. P. Adhikari, *J. Molec. Liq.* **194**, 77 (2014).
11. D. Frenkel and B. Smit, *Understanding Molecular Simulation From Algorithms to Applications* (Academic Press, USA, 2002).
12. M. P. Allen and D. J. Tildesley, *Computer Simulation of Liquids* (Oxford University Press, USA, 1989).
13. V. Ballenegger, S. Picaud and C. Toubin, *Chem. Phys. Lett.* **432**, 78 (2006).
14. L. S. Darken, *AIME* **175**, 184 (1948).
15. D. van der Spoel et al., *Gromacs User Manual version 4.5.6* (2010).
16. www.mrbigler.com/misc/Pvap-H2O.PDF.
17. D. A. McQuarrie, *Statistical Mechanics* (University Science Books, USA, 2000).
18. D. L. Wise and G. Houghton, *Chem. Eng. Sci.* **23**, 1213 (1968).
19. D. L. Wise and G. Houghton, *Chem. Eng. Sci.* **21**, 999 (1966).
20. A. J. Easteal, W. E. Price and L. A. Woolf, *J. Chem. Soc. Faraday Trans.* **1**, 85 (1989).
21. I. G. Zacharia and W. M. Deen, *Ann. Biomed. Eng.* **33**, 214 (2005).
22. T. Malinski, Z. Taha and S. Grunfeld, *Biochem. Biophys. Res. Commun.* **193**, 1076 (1993).
23. K. Sharma and N. P. Adhikari, *Int. J. Mod. Phys. B* **28**, 14 (2014).